Journal of Positive School Psychology
2022, Vol. 6, No. 3, 5368–5379 http://journalppw.com

Formulation And Characterization Of Polymeric Nanoparticles For Enhancing Bioavailability Of Herbal Anticancer Castalin

J.Praveen kumar[1], Dr.P.Geetha[2*]

[1]*Research Scholar, Vel's Institute of science and Technology advanced studies (VISTAS), Chennai-600117, Tamilnadu, India.*
jalduppraveen@gmail.com
[2]*Assistant Professor, Vel's Institute of science and Technology advanced studies (VISTAS), Chennai-. 600117, Tamilnadu, India.*
lgeethapharma@gmail.com

Corresponding Author:
Dr.P.Geetha,
Email: lgeethapharma@gmail.com
Mobile no: 9940460178

Abstract

The destiny look at entails delivering drug/bioactive based totally on a unmarried nanoplatform poly lactic-co- glycolic acid (PLGA) for superior efficacy, synergistic effect, and reduced toxicity. Diverse NP formulations were allotted in drug development in an try to growth performance, protection and tolerability of integrated tablets. In this context, NP formulations that increase solubility, control release, and/or affect the in vivo disposition of drugs, had been evolved to enhance the pharmacokinetic and pharmacodynamic homes of encapsulated drugs. The nanoparticles have been formulated further to then characterized for percent yield, encapsulation performance, surface morphology, particle dimension, drug distribution studies, drug polymer interaction research and in vitro drug launch profiles. The goal of this effort is to put together and compare Poly (D, L-Lactide-co-glycolide) (PLGA) Nanoparticles (NPs) of Castalin, an anticancer agent loaded by solvent displacement method by stabilizer (poly vinyl alcohol). The set NPs were characterized by FT-IR, DSC, drug loading, entrapment efficiency, particle size, and surface morphology by Atomic force microscopy (AFM), X-ray diffraction and in-vitro studies. FT-IR and DSC research indicated that there was no interplay between the drug and polymer. The morphological studies executed by using AFM showed uniform and spherical fashioned discrete particles without aggregation and easy in surface morphology with a nano length varies of 144 nm. The enormous quantity of news on PLGA NPs used as drug delivery systems during cancer management effects to see the potential of PLGA NPs used as drug delivery systems in the course of most cancer therapeutics and encourages similarly translational research.

Keywords: Nanoparticles; PLGA; Castalin; most cancers; sustained release; goal transport.

Introduction

The narration of plants being used since medicines is thousands of years old and in the case of cancer about 60% of anticancer drugs arrive from either natural supplies or derivatives of natural supplies.1 Natural products encompass a wealthy source of new chemical entities while a drug innovation platform.2 Reports indicated that 34% of small molecules including anticancer drugs with the purpose of have be approved as new medicines by US Food and Drug Administration (FDA) among 1981 and 2010 were either natural products or derivatives of natural products.2–5 The gum tannin obtained from *Malaleuca*

quinquenervia leaves., which is a deciduous plant, widely distributed in the dry region of China and India.

Presently, there are many types of polymers available in support of polymer based NP formulation. Examples of common polymers employed in NP formulation are poly (lactic acid) (PLA), poly (glycolic acid) (PGA), as well as poly (lactic-co-glycolic acid) (PLGA) *(Cooper et al 2014)*. Like numerous NP delivery systems, polymer based NP formulation can act to offset drug release by desorption of bound drug from particle surfaces, erosion of the polymer membrane, and/or drug diffusion *(Buzea et al 2007; Dejong and Borm 2008; Cooper et al 2014)*. The three abovementioned stages next to which polymer NPs can liberate active pharmaceutical agents makes them an ideal choice in attempting to formulate a innovative and novel drug delivery systems that could act to modify or else control drug release and offset the occurrence of drug related adverse events.

Materials and Methods:

Castalin PLGA (lactide/glycolide = 50:50, Resomer® 503H) was purchased from Boehringer Ingelheim Pharma Gmbh & Co. Germany. Tocopheryl polyethylene glycol succinate (TPGS) and Acetone were obtained from Sigma Aldrich, India.

Ellagitannins differ from gallotannins, during to facilitate their galloyl groups are linked through C-C bonds, whereas the galloyl groups in gallotannins are linked by depside bonds. It can be found in oak wood and Melaleuca quinquenervia is botanical name and family Myrtaceae.

Preparation of Castalin NPs

Castalin loaded PLGA nanoparticles have been organized through nanoprecipitation approach. In short, by dissolving 100 mg of PLGA changed into dissolved in 1 mL of acetone and then introduced drop clever to 10 mL of TPGS solution (0.3 % w/v) with continuous stirring. Castalin 10 mg turned into dissolved 10 ml of water. Organic section obtained with the addition of PLGA and TPGS solution in acetone changed into introduced drop clever to aqueous segment of Castalin solution upon stirring. Acetone turned into allowed evaporating through continuous magnetic stirring for 4 h. Castalin loaded PLGA nanoparticles were then recovered from the nano-dispersion with the aid of centrifugation at 15,000g force for 35 min at 4°C. Then, brought about precipitated PLGA nanoparticles have been suspended in mannitol solution (5% w/v) and lyophilized for 72 h.

Experimental design

Particle size, size distribution, and system yield and entrapment efficiency of the Castalin nanoparticles. For this reason, a central composite rotatable design–response surface methodology (CCRD–RSM) was used to systemically investigate the influence of these three critical formulation variables on particle size, % yield and % entrapment efficiency (EE) of the arranged nanoparticles. The details of the design are listed in **Table 1**. The value range of the variables be drug polymer ratio (X1) of 1:1 to 1:7, ratio of aqueous to organic phase (X2) of 1:1–1:5 and stirring time (X3) of15 to 45 min. A complete of 20 tests had been conducted. All the formulations in those experiments have been organized in replica.

Characterization of the NPs

Particle size, Polydispersibility index and Zeta potential:

Particle size evaluation changed into carried out by using dynamic light scattering (DLS) with a Malvern Zetasizer 3 000 HSA (Malvern Instruments, UK). The mean diameter and PI values were obtained at an angle of 90° in 10 mm diameter cells at 25 °C. Prior to the measurements all samples have been diluted with double distilled water to produce a appropriate scattering depth.

Zeta potential

The zeta potential, reflecting the electric charge on the particle surface and indicating the physical stability of colloidal systems, was measured by determining the electrophoretic mobility using the Malvern Zetasizer 3 000 HSA (Malvern Instruments, UK). The sample was measured in double distilled water and adjusted to a conductivity of 50 IS/cm with sodium chloride solution (0.9% w/v). The pH

was in the range of 5.5–7.5 and the applied field strength was 20 V/cm.

Scanning electron microscopy (SEM) measurement

The samples for scanning electron microscope (SEM) were mounted on metal stubs and the surface and surface morphology of the particles were examined by a Hitachi S4800 Field Emission Scanning Electron Microscope (Hitachi, Gaithersburg, MD, USA). The analytical parameters included an accelerating voltage of 10 KeV, a working distance of 13.5 mm, and a vacuum of 40 Pascals.

Differential Scanning Calorimetry (DSC) analysis

A differential scanning calorimeter (DSC) (Shimadzu DSC-60, Columbia, MD, USA) was used to analyze pure Castalin, PLGA, and physical mixture and Castalin nanoparticles. The sample to be analyzed (3–5 mg) by DSC was crimped nonhermetically in an aluminium pan and heated from room temperature (23°C) to 300°C at a rate of 10°C/min under nitrogen purge.

Fourier Transmission Infrared spectroscopy (FTIR) analysis

FTIR analyses of Castalin, PLGA, physical combination and Castalin nanoparticles have been carried out using IR Prestige-21 (Shimadzu, Columbia,MD, USA). The sample was placed in direct contact with ATR crystal ensuring good contact. All the spectra were recorded when a mean of20 scans, among a resolution of 4 cm-1 and during the range of 800 to 4000 cm-1.

Chromatographic conditions

The awareness of Castalin become detected by means of high-performance liquid chromatography (HPLC) system the usage of a C18 Luna column5-µm particle size, 25 cm×3.00 mm I.D. (Phenomenex, Torrance, CA, USA).A mobile phase composed by water–formic acid (99.5:0.5, v/v) (solvent A) and acetonitrile (solvent B) was used. The flow rate was 0.5ml/min. The injection volume was 10 µL and the wavelength was set at 246 nm.

Determination of drug entrapment efficiency (EE) and process yield

This gives the quantity of drug this is unentrapped within the nanoparticles. Quantity of drug located in the supernatant was subtracted from the total amount of drug added to the formulation which gives the amount of drug entrapped in the nanoparticles. The formulations were evaluated for entrapment efficiency by the following formula

$$EE = \frac{Mass\ of\ drug\ in\ nanopartilce}{Mass\ of\ drug\ used\ in\ the\ formulation} \times 100\%$$

Progression yield

The yield of nanoparticles were calculated using the following equation

$$Yield = \frac{Mass\ of\ nanoparticles\ recovered}{Mass\ of\ polymer + drug + excipients} \times 100$$

In vitro release study

100 ml of Phosphate buffer, pH adjusted to 7.4 was poured into a well-closed glass vessel as the dissolution medium intended the in vitro release test. Castalin nanoparticle (5 ml) was transferred to a dialysis bag (molecular weight cut-off 5000–10,000) and then the dialysis bag The vessels were placed in an incubator shaker and shaken horizontally (Incubator Shaker ZHWY-200B, Shanghai ZhichengAnalysis Instrument Company, China) at 37 °C and 100 strokes per min. The sample (1 ml) was withdrawn from the system at predetermined time intervals and filtered through a 0.45 µm hydrophilic filter membrane. The drug content was measured by the HPLC method described above. The diffusion profile of pure drug suspension through a dialysis bag was examined as control. The pure drug suspension was prepared by dispersing 1 ml Castalin solution (5 mg/ml) in 4 ml of double distilled water was placed in the glass vessel.

Storage stability

The storage stability of optimized nanoparticles were determined as follows. Briefly, an aliquot of 15 ml nanoparticles suspension with 1 mg/ml drug concentration was placed into glass vials and stored at 4 and 25 ℃ in the dark for 180 days, and the changes of particle size and zeta potential against storage time were investigated. Furthermore, drug entrapment efficiency (EE) against storage time was determined under 4 °C. Prior to the measurement of particle size, zeta potential and entrapment efficiency, the nanoparticles powders were re-dispersed in distilled water with 1 mg/ml drug concentration by vortexing for 3 min. The nanoparticles establish follows as particle sizes, zeta potential values, entrapment efficiency.

Data analysis

The interaction related to responses and formulation variables of all model formulations were treated by Design-Expert® software. Statistical analysis including stepwise linear regression and response surface analysis was conducted. The significant terms ($p<0.05$) were chosen for final equations. Suitable models consisting of three components include linear, quadratic and special cubic models. The best fitting mathematical model was selected based on the comparisons of several statistical parameters including the coefficient of variation (c.v.), the multiple correlation coefficient (R2), and the adjusted multiple correlation coefficient (adjusted R2) proved by Design-Expert software. Significance of differences was evaluated using Student's t-test and one way ANOVA at the probability level of 0.05.

Results & Discussion

The central composite rotatable design–response surface methodology (CCRD–RSM) constitutes an alternative approach because it offers the possibility of investigating a high number of variables at different levels with only a limited number of experiments. . The variables in **Table 1** were chosen taking into account our preliminary experiments. **Table 2** showed the experimental results concerning the tested variables on drug entrapment efficiency, process yield, and mean diameter of particle size. The three dependent values ranged from 80 to 91% by weight, 61 to 93% by weight, and 150 to 201 nm. A mathematical relationship between factors and parameters was generated by response surface regression analysis using Design-Expert® 7.0 software. The three-dimensional (3D) response surface graphs for the most statistical significant variables on the evaluated parameters are shown in **Fig. 1 –4.** The response surface diagrams showed that an increase in polymer concentration and aqueous to organic phase ratio increases the particle size and entrapment efficiency. Process yield of nanoparticles decreases at a stage increasing both the polymer concentration and aqueous to organic phase ratio. The optimized variables showed a good fit to the second-order polynomial equation, with correlation coefficient (r) of 0.9627, 0.7514 and 0.7198 respectively. After model simplification with backward stepwise solution, the r value decreased slightly to 0.9387, 0.6454 and 0.5055 respectively. The lack off it was not significant at 95% confidence level. All the remaining parameters were significant at $p\leq0.05$. It was observed that the best fitted model was the quadratic model, and the comparative values of R, SD and % CV along with the regression equation generated for the selected responses are given in **Table 3**. The statistical analysis of the results generated the following polynomial equations:

The fitting results indicated that the optimized nanoparticles with high EE, high yield and small mean diameter was obtained at the drug polymer ratio of 1:1, aqueous to organic phase ratio of 1:5and stirring time of 21min respectively. **Table 4** showed that the experimental values of the two batches prepared within the optimum range were very close to the predicted values, with low percentage bias, suggesting that the optimized formulation was reliable and reasonable. Perturbation plots in **Figure 5-7** reveals the impact of an independent factor on a particular response, with all various other aspects held consistent at a referral factor. A steep incline or curvature suggests sensitiveness of the response to a specific factor. **Figure 5** shows that stirring time had one of the most crucial impact on particle size followed by aqueous to organic phase ratio and drug polymer ratio. **Figure 6** shows that stirring time had one of the most crucial impact on entrapment efficiency followed by aqueous to organic

phase ratio and drug polymer ratio. **Figure 7** reveals that aqueous to organic phase ratio had the most crucial result on process yield followed by stirring time and drug polymer ratio.

Table 1. Independent variables and their corresponding tiers of nanoparticle preparation

Independent variables	Levels		
	-1	**0**	**+1**
Drug/polymer ratio	1:1	1:4	1:7
Aqueous to organic phase ratio	1:1	1:3	1:5
Stirring time	15	1:30	45

Table 2. Central composite rotatable design generated through Design Expert 11® software along with the obtained response

Std	Run	Factor 1 A:Drug Polymer	Factor 2 B:Aqueous to organic	Factor 3 Stirring time min	Response 1 Particle size nm	Response 2 Entrapment efficiency %	Response 3 Process yield %
15	1	4	3	30	210	90	90
20	2	4	3	30	208	92	80
7	3	1	5	45	173	93	72
2	4	7	1	15	176	90	66
11	5	4	-0.1654	30	191	84	74
17	6	4	3	45	210	92	80
8	7	7	5	30	180	93	64
12	8	4	5.1321	30	161	92	80
16	9	4	2	30	210	92	80
18	10	4	3	25	208	90	90
5	11	1	1	45	184	90	87
13	12	4	5	4.734	170	83	60
4	13	7	3	15	160	84	80
19	14	4	2	30	250	92	68
3	15	1	2	15	153	87	76
1	16	1	3	15	172	90	67
9	17	-1.0038	3	30	167	92	54
6	18	7	1	45	159	83	55
14	19	4	2	55.224	189	90	66
10	20	8.645	3	30	186	83	77

Table 3. Decreased response models and statistical parameters received from ANOVA

Responses	Regression model	Adjusted R^2	Model P value	%CV	Adequate precision
Particle size	PS = 210.10-2.16A-4.45B+5.63C+4.37AB-4.38AC+6.37BC-14.28A^2-11.98B^2-11.45C^2	0.9337	0.0001	2.65	17.57
Entrapment efficiency	EE% = 91.10-2.06A+0.9585B+1.49C+1.37AB-0.3750AC+3.13BC	0.6424	0.0001	2.41	10.04

Process yield	Yield % = 90.30-1.20A+1.55B-0.3628C-3.25AB+2.75AC-1.50BC-9.71A^2-2.46B^2-2.46C^2	0.5015	0.0001	3.12	24.05
Acceptance criteria		1	<0.05	<4	>10

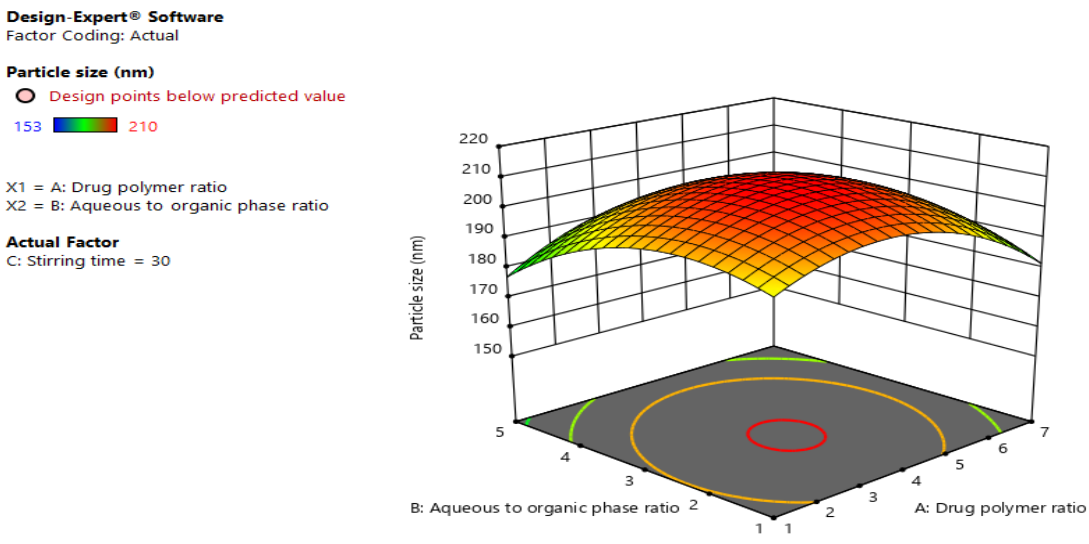

Figure 1: 3-dimensional (3-d) response surface plots showing the effect of the variable on response. The effect of drug/polymer ratio and aqueous to organic phase ratio on particle size

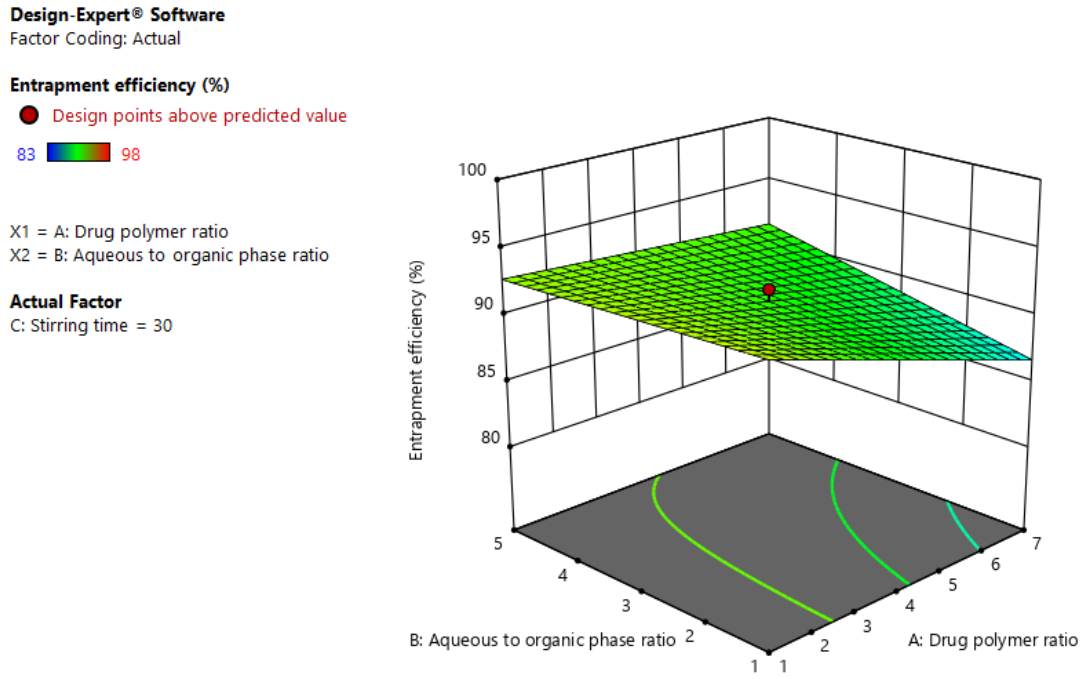

Figure 2: 3-dimensional (3-d) response surface plots displaying the effect of the variable on response. The effect of drug/polymer ratio and aqueous to organic phase ratio on entrapment efficiency

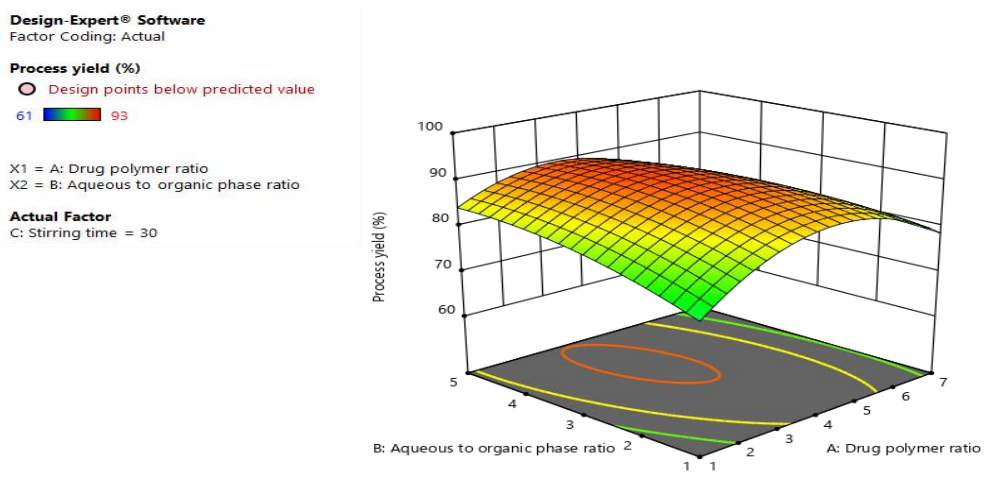

Figure 3: 3-dimensional (3-d) response surface plots showing the effect of the variable on response. The effect of drug/polymer ratio and aqueous to organic phase ratio on process yield

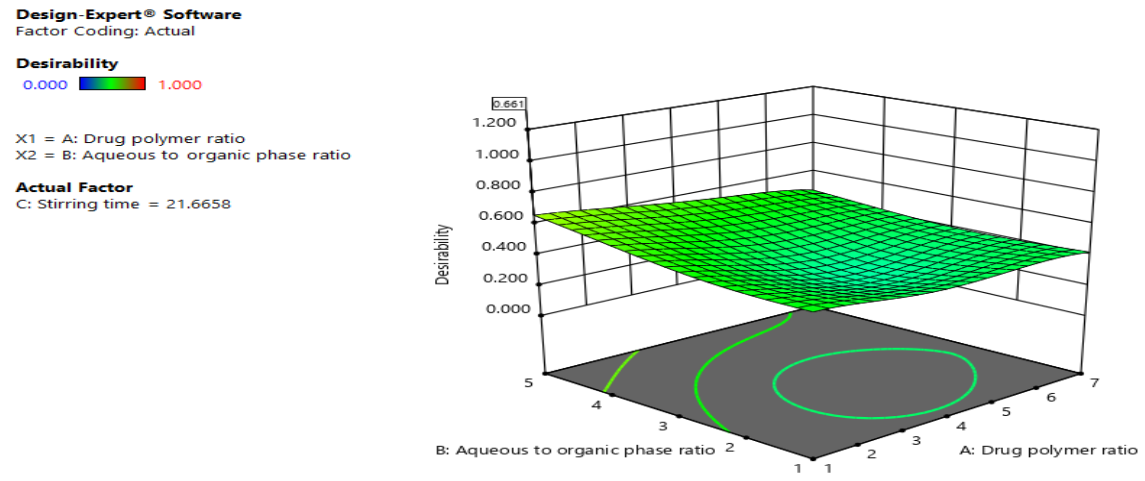

Figure 4: 3-dimensional (3-d) response surface plots showing the desirability with a cost of 0.66

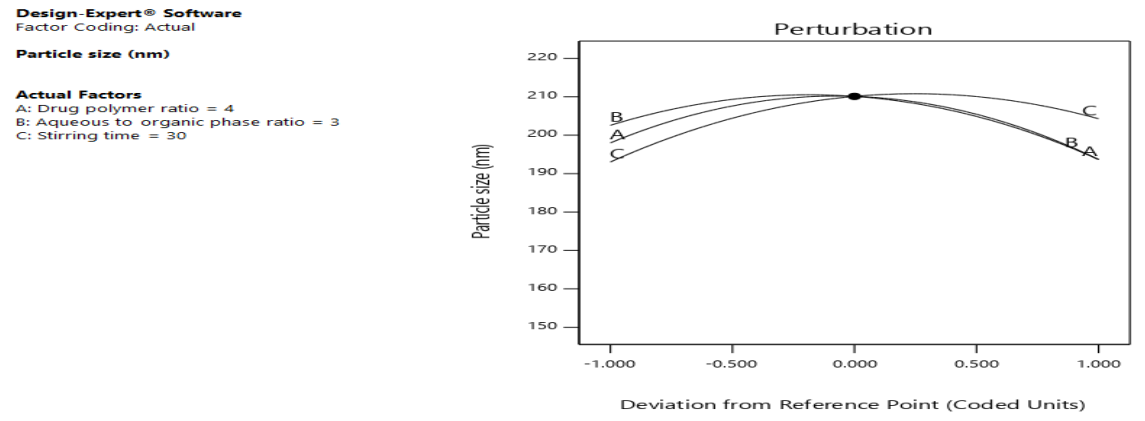

Figure 5: Perturbation plot showing the impact of each of the unbaised variables on Particle size in which A, B and C are Drug/polymer ratio, aqueous to organic phase ratio and stirring time respectively

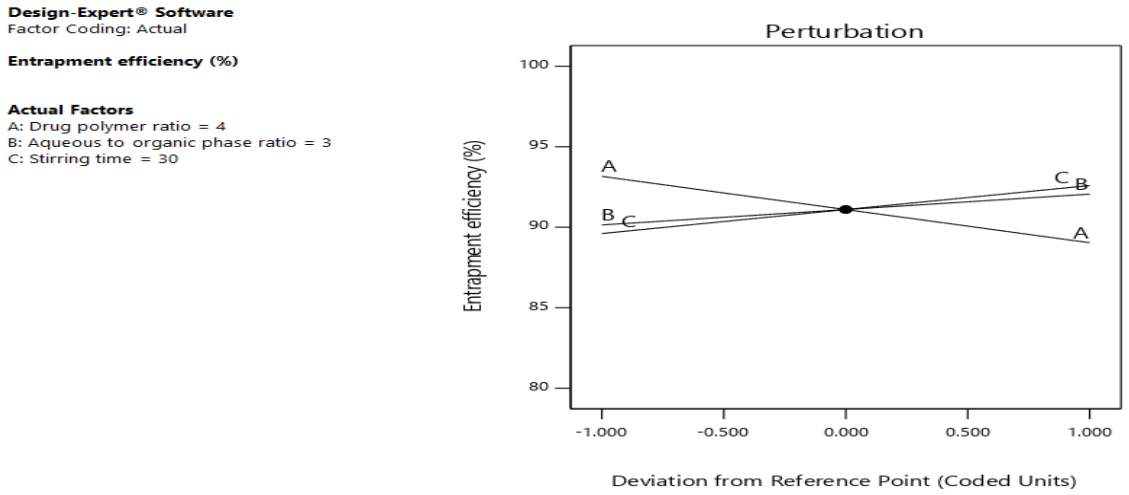

Figure 6: Perturbation plot showing the impact of each of the unbiased variables on entrapment efficiency wherein A, B and C are Drug/polymer ratio, aqueous to organic phase ratio and stirring time respectively

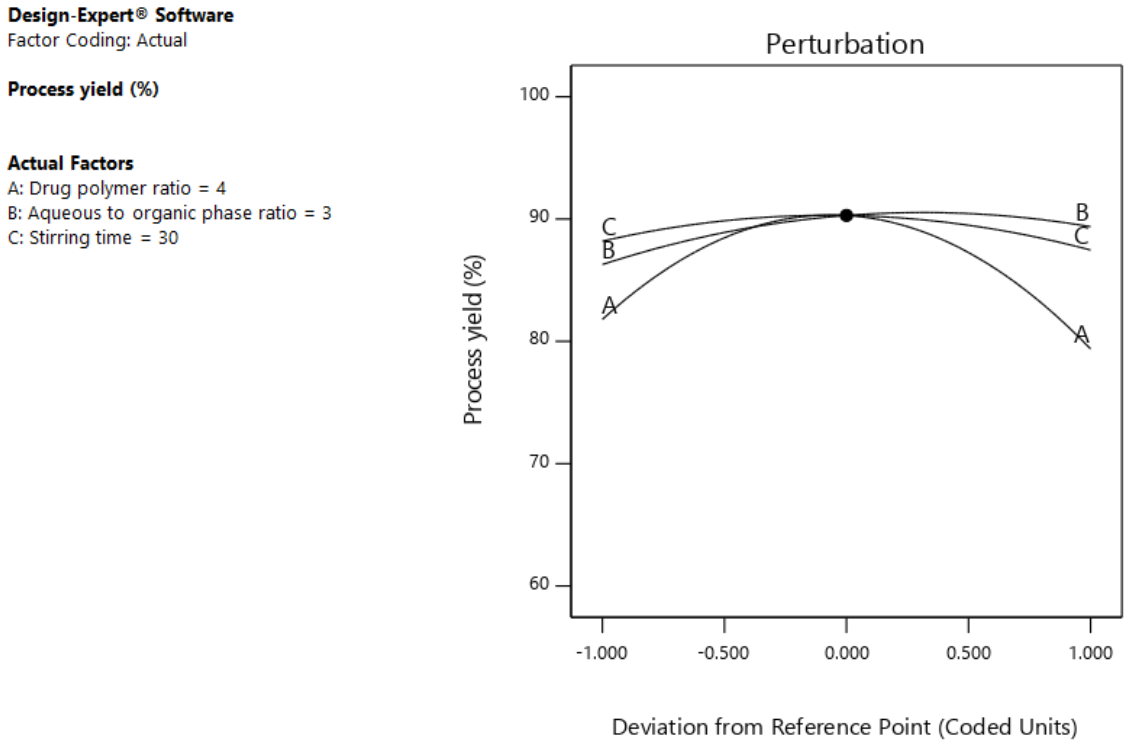

Figure 7: Perturbation plot showing the effect of each of the unbaised variables on technique yield where A, B and C are Drug/polymer ratio, aqueous to organic phase ratio and stirring time respectively

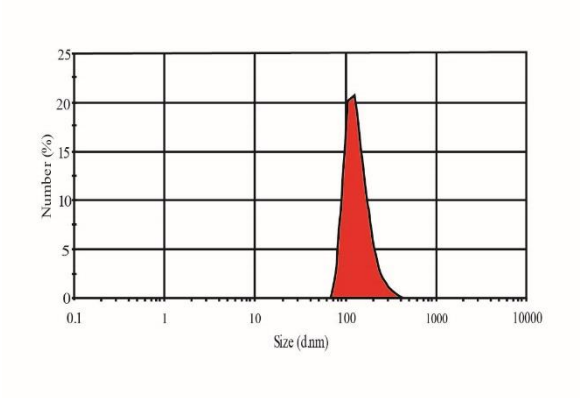

Figure 8: Particle size of optimized Castalin nanoparticles

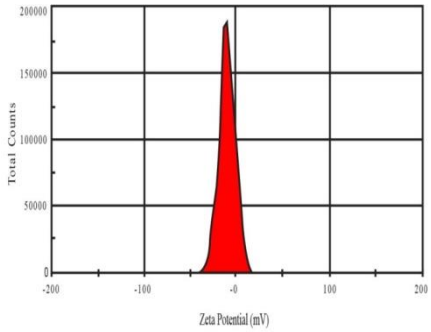

Figure 9: Zeta potential of optimized Castalin nanoparticles

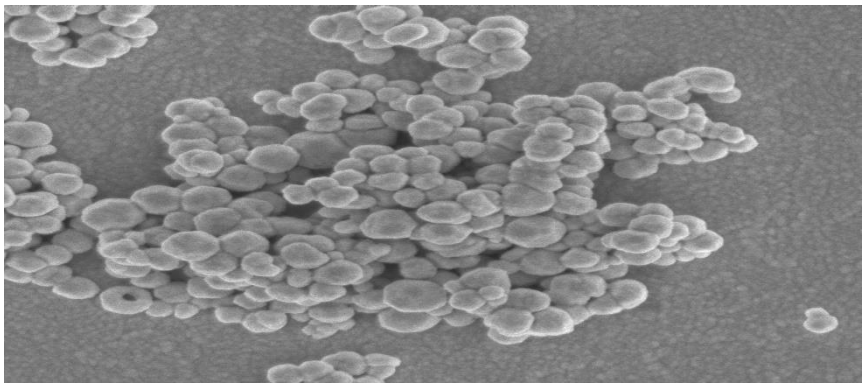

Figure 10. SEM photograph of optimized Castalin nanoparticles

Differential Scanning Calorimetry (DSC) analysis

DSC was performed to analyze the physical state of Castalin within the PLGA nanoparticles upon the preparation. Thermogram of PLGA showed a pointy endothermic peak at 40-60°C **(Figure 11).** The pure Castalin shows a sharp endothermic peak that corresponds to melting point at 210-215°C. The illustration of the weak peaks obtained corresponding to Castalin in the DSC thermogram of the nanoparticles suggests that the drug is well dispersed in the formulation

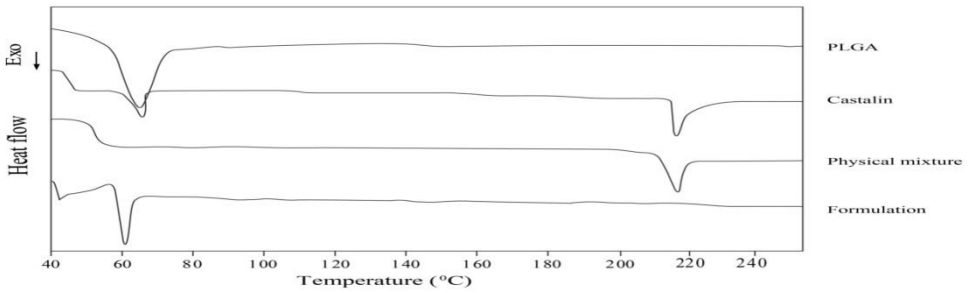

Figure 11. DSC of Castalin, PLGA, physical mixture and nanoformulation

Fourier Transmission Infrared spectroscopy (FTIR) analysis

FTIR analysis is used to have a look the interactions between Castalin, PLGA, physical mixture and the drug loaded nanoparticles and the spectrum obtained is presented in Figure 12. The IR of the aggregate of drug sample and PLGA were found to be within the specified range. Hence there is no interaction between the drug sample and PLGA and can be well used in the formulation. Castalin procured their entire characteristic peak in physical mixture. That is significant peak 750-1580 were retained in the physical mixture. Peak at 2890 and 3100 have been prominent in Castalin alongside the physical mixture. In fingerprint region of Castalin the characteristic band at 850 and 1350-1580 were retained in the physical mixture. On the basis of FTIR spectra investigation no chemical interplay were found between Castalin and PLGA

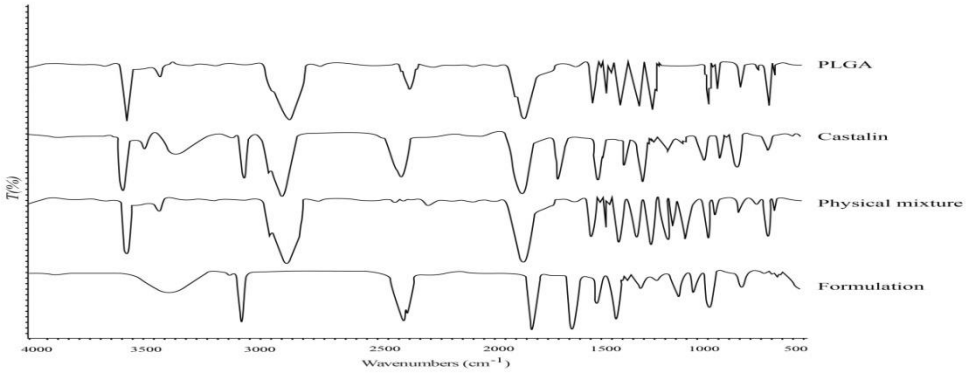

Figure 12. FTIR of Castalin, PLGA, physical mixture and nanoformulation

Table 4. Assessment of experimental and predicted values underneath greatest conditions for very last system

Drug/polymer ratio	Aqueous to organic phase ratio	Stirring time (min)	Particle size (nm)	Entrapment efficiency (%)	Process yield (%)
1:1	1:5	21.66			
Predicted			161	86.9	84.9
Experimental			159	88.0	84.0
Bias %			0%	1.0%	1.0%
Acceptance criteria 6%					
Bias was calculated as (predicted value - experimental value)/predicted value × 100					

In vitro drug launch observe

The in vitro release overall performance of Castalin from the solution and nanoparticles were studied for greater than 24 h as proven in **Figure 13**. Because it was shown, drug release from the solution and the nanoparticles occurred in a biphasic way of burst release and sustained launch. Due to the burst effect, the drug from the solution was released fast and finished in 24 h. It was located that there has been an preliminary burst launch in keeping with the accumulative release rate of Castalin from the nanoparticles, in addition to this result can be because of Castalin adhered on the surface of the nanoparticles. A sustained Castalin release to about 72 % was possessed for the nanoparticles over 12 h. as a result, the polymer PLGA prevents the Castalin burst release and controls the release rate of Castalin. moreover, in vitro launch curve advise that Castalin nanoparticles possessed a extraordinary time prolongation impact on Castalin release and helps long time stability.

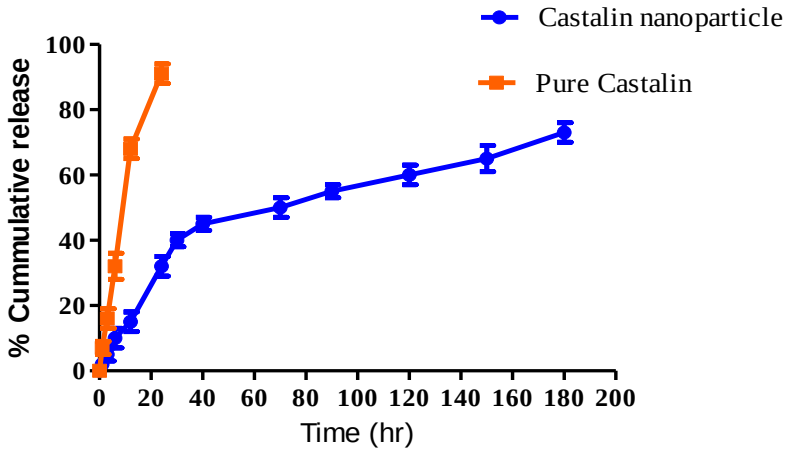

Figure 13. Cumulative Percentage drug release of pure drug Castalin and Castalin nanoparticles in PBS (pH 7.4)

Discussion

Numerous investigations have been performed at growing greater green structures for drug delivery. The maximum vital assignment inside the a hit system of polymeric drug transport systems includes preparing carrier structures which are that are able to encapsulating the desired drug inside its structure and then deliver the drug to the cancerous tissues in its active form. The formulation of synthesizing drug loaded polymeric nanoparticles involves preparation and characterization of drug encapsulated nanoparticles The fate of a drug after administration *in vivo* depends primarily on the physicochemical properties of the drug and on its chemical structure, therefore physicochemical characterization of drug loaded nanoparticles system becomes essential. Particle size is an important parameter as it can directly affect the physical stability, cellular uptake, and biodistribution and drug release from the nanoparticles. Our formulation of Castalin-loaded PLGA nanoparticles by using the nanoprecipitation resulted in particles with high Castalin encapsulation (~91%) with a size range of 35-100 nm. Other studies have reported different Castalin formulations such asmicellar aggregates

Conclusion

In this take a look at, Castalin -loaded PLGA nanoparticles had been organized by way of the nanoprecipitation approach. Our research confirmed that clean, round PLGA nanoparticles have been formed and exhibited excessive yield and drug entrapment efficiency, with a slender length variety of 33 nm to 102 nm and mean particle diameter of 43 nm. The *in vitro* Castalin launch studies from the nanoparticles confirmed that Castalin turned into released in a sustained way over a

extended time frame. Intracellular uptake and cell viability assays also verified green uptake and action of the Castalin nanoparticles in prostate cancer cell strains. It is therefore concluded that PLGA nanoparticles are capable of delivering Castalin over a extended duration accomplishing a sustained transport of Castalin, hence making it a potential candidate for cancer remedy.

References

Aggarwal BB, Kumar A and Bharti AC: Anticancer potential of curcumin: preclinical and clinical studies. Anticancer Res 23: 363-398, 2003.

Buzea et al 2007; Dejong and Borm 2008; Cooper et al 2014 Nanoparticles in drug delivery: mechanism of action, formulation and clinical application towards reduction in drug-associated nephrotoxicity, 2014 - Issue 10

Duvoix A, Blasius R, Delhalle S, Schnekenburger M, Morceau F, Henry E, Dicato M and Diederich M: Chemopreventive and therapeutic effects of curcumin. Cancer Lett 223: 181-190, 2005.

Gordon EM, Cornelio GH, Lorenzo CC III. First clinical experience using a 'pathotropic' injectable retroviral vector (Rexin-G) as intervention for stage IV pancreatic cancer. Int J Oncol 2004; 24:177-85.

Maheshwari RK, Singh AK, Gaddipati J and Srimal RC: Multiple biological activities of curcumin: a short review. Life Sci 78: 2081-2087, 2006.

Neha S, Viness P, Yahya E. Advances in the treatment of Parkinson's disease. Prog Neurobio 2007; 81(1):29-44.

Ram B Gupta, Uday B. Kompella. Nanoparticle technology for drug delivery. New York: Taylor & Francis Group; 2006: p. 273-4.

Ramsey L B, Johnson S G, Caudle K E, Haidar C E, Voora D, Wilke R A, Maxwell W D, McLeod H L, Krauss R M, Roden D M, Feng Q, Cooper R M -DeHoff,L Gong,T E Klein, Wadelius M, Niemi M The Clinical Pharmacogenetics Implementation Consortium Guideline for SLCO1B1 and Simvastatin-Induced Myopathy: 2014 Update Pages 423-428

Rockall AG, Sohaib SA, Harisinghani M. Diagnostic performance of nanoparticle-enhanced magnetic resonance imaging in the diagnosis of lymph node metastases in patients with endometrial and cervical cancer. J Clin Oncol 2005; 23:2813-21.

Shishodia S, Sethi G and Aggarwal BB: Curcumin: getting back to the roots. Ann N Y Acad Sci 1056: 206-217, 2005.

Wang Z, Zhang Y, Banerjee S, Li Y and Sarkar FH: Notch-1 down-regulation by curcumin is associated with the inhibition of cell growth and the induction of apoptosis in pancreatic cancer cells. Cancer 106: 2503-2513, 2006.